PHYSICAL REVIEW C VOLUME 14, NUMBER 3 SEPTEMBER 1976

Decay schemes for high-spin states in ^{35,36,37}Cl and ^{37}Ar from heavy-ion fusion-evaporation reactions*

E. K. Warburton, J. W. Olness, A. R. Poletti,† and J. J. Kolata
Brookhaven National Laboratory, Upton, New York 11973
(Received 4 May 1976)

The γ-ray decays of high-spin states in ^{35,36,37}Cl and ^{37}Ar were studied via heavy-ion-induced reactions involving ^{14}N and ^{18}O bombardment of targets of ^{24,26}Mg and ^{27}Al. Decay schemes and spin-parity assignments were deduced from $\gamma\gamma$-coincidence measurements, γ-ray angular distribution and linear polarization measurements, and recoil-distance lifetime measurements. The observed levels are compared to predictions of the weak-coupling model. It is concluded that all the observed high-spin states can be assigned to configurations based on one- or two-nucleon excitations from the $(2s,1d)$ shell into the $(1f,1p)$ shell, and that not all the energetically available yrast levels of these configurations have, as yet, been found.

NUCLEAR REACTIONS (HI, xn, yp, $z\alpha$) studies for ^{35,36,37}Cl and ^{37}Ar, with ^{14}N, ^{18}O projectiles, ^{24,26}Mg and ^{27}Al targets, E =20–60 MeV; measured $\gamma\gamma$ coin.; deduced levels; measured $\sigma(E_\gamma, \theta)$ and P_γ; deduced J^π for high-spin levels; measured recoil distance; deduced τ. Natural and isotopically enriched targets, Ge(Li) detectors. Compared results to weak-coupling model predictions.

I. INTRODUCTION

In the last few years our knowledge of the spectroscopy of the low-lying high-spin states of nuclei in the region of $A \lesssim 60$ has been considerably extended by the use of in-beam γ-ray spectroscopy utilizing (α,n) and (α,p) reactions on the one hand and heavy-ion fusion-evaporation reactions on the other. In the heavy-ion (HI) induced reaction there are many open exit channels, i.e., in the reaction denoted by $(\mathrm{HI},xn,yp,z\alpha)$—$x,y,z$ take on all permutations of values between 1 and 3 with a practical limit $x+y+z \lesssim 4$. Since for all of these exit channels the cross section is large in the projectile energy range 30–60 MeV where the majority of the studies have taken place, the reaction is not very selective but is a very good survey tool. In addition, the large energy excess (highly exothermic reactions) results in a quite weak dependence on beam energy of the relative cross section for forming different high-spin states in a given nucleus.

In contrast, the α-induced reaction is selective not only because the (α,n) and (α,p) reactions dominate but also because the endothermic nature of the reaction to the higher-lying high-spin states causes the cross section to a particular level to be strongly energy dependent with a rather sharp threshold. For these and other reasons, the (α,n) and (α,p) reactions are more suitable for the detailed study of those states accessible by both α-induced and HI-induced reactions. However, the fusion-evaporation reaction is an excellent survey tool and, quite importantly, appears to form higher-lying yrast levels that have not been seen in the (α,n) and (α,p) reactions.

This latter point and the utilization of the fusion-evaporation reaction in nuclear spectroscopy surveys is illustrated by the results presented here

TABLE I. List of fusion-evaporation studies with compound nuclei having $A \leq 47$.

Identification No.	Projectile	Target	Compound nucleus	E_x [a] (MeV)
1	^{18}O	^{24}Mg	^{42}Ca	46.68
2	^{19}F	^{24}Mg	^{43}Sc	43.08
3	^{18}O	^{26}Mg	^{44}Ca	48.10
4	^{18}O	^{27}Al	^{45}Sc	47.08
5	^{19}F	^{26}Mg	^{45}Sc	46.47
6	^{19}F	^{27}Al	^{46}Ti	48.92
7	^{14}N	^{26}Mg	^{40}K	46.18
8	^{16}O	^{27}Al	^{43}Sc	39.36
9	^{14}N	^{27}Al	^{41}Ca	47.13
10	^{19}F	^{28}Si	^{47}V	42.86
11	^{18}O	^{25}Mg	^{43}Ca	41.17
12	^{13}C	^{26}Mg	^{39}Ar	33.48
13	^{12}C	^{26}Mg	^{38}Ar	31.14
14	^{12}C	^{25}Mg	^{37}Ar	30.73
18	^{18}O	^{18}O	^{36}S	49.09
19	^{16}O	^{18}O	^{34}S	43.24
22	^{12}C	^{19}F	^{31}P	38.44
23	^{13}C	^{18}O	^{31}Si	42.08
24	^{12}C	^{18}O	^{30}Si	39.66
25	^{13}C	^{16}O	^{29}Si	38.21
29	^{18}O	^{10}Be	^{28}Mg	52.56
32	^{11}B	^{12}C	^{23}Na	39.07
35	^{13}C	^{10}Be	^{23}Ne	43.49

[a] E_x is the excitation energy of the compound nucleus at a bombarding energy of 40 MeV.

TABLE II. Relative intensities of specific final nuclei resulting from decay of the indicated compound nuclei.

Identification No.	Compound nucleus	E_x [a] (MeV)	^{35}Cl Channel	^{35}Cl Intensity [b]	^{36}Cl Channel	^{36}Cl Intensity [b]	^{37}Cl Channel	^{37}Cl Intensity [b]	^{37}Ar Channel	^{37}Ar Intensity [b]
14	^{37}Ar	30.73	pn	35	p	≤1	...	...	...	...
13	^{38}Ar	31.14	$p2n$	34	pn	44	p	1	n	≤1
12	^{39}Ar	33.48	$p3n$	8	$p2n$	116	pn	14	$2n$	15
7	^{40}K	46.18	αn	42	α	26	$2pn$	44	$p2n$	184
9	^{41}Ca	47.13	αpn	96	αp	73	$3pn$	...	α	9
1	^{42}Ca	46.68	$\alpha p2n$	...	αpn	80	αp	20	αn	37
11	^{43}Ca	39.72	$\alpha p3n$	...	$\alpha p2n$	...	αpn	16	$\alpha 2n$	78
8	^{43}Sc	39.36	2α	65	$\alpha 2pn$	...	$\alpha 2p$	6	αpn	33
2	^{43}Sc	43.08	2α	21	$\alpha 2pn$	...	$\alpha 2p$	6	αpn	37
3	^{44}Ca	48.10	$\alpha p4n$	...	$\alpha p3n$	...	$\alpha p2n$	...	$\alpha 3n$	...
5	^{45}Sc	46.47	$2\alpha 2n$	...	$2\alpha n$	21	2α	5	$\alpha p3n$	≤2
4	^{45}Sc	47.08	$2\alpha 2n$	...	$2\alpha n$	25	2α	8	$\alpha p3n$	≤2
6	^{46}Ti	48.92	$2\alpha p2n$	...	$2\alpha pn$	...	$2\alpha p$	3	$2\alpha n$	28
10	^{47}V	45.84	3α	5	$2\alpha 2pn$	...	$2\alpha 2p$	...	$2\alpha pn$	2

[a] The E_x corresponds to bombarding energies $E_B = 45$ MeV (ID 10) and 37.5 MeV (ID 11); for all others $E_B = 40$ MeV (see Table I).

[b] The data are normalized so that for each projectile-target combination the γ transitions for all reactions have an *average* strength of 10 units (arbitrary). The intensities are the total γ-ray flux leading into the ground state. The uncertainties on the quoted intensities are ±25%.

TABLE III. ^{35}Cl γ rays observed in fusion-evaporation reactions.

γ-ray energy [b] (keV)	Relative [c] intensity	Angular distribution [a] A_2 (%)	A_4 (%)
[160.66(20)]	1408	−24(15)	0
517.26(10) [d]	(1330)	47(25)	0
680.22(15) [e]	15 213	−20(2)	0
882.42(35)	1421	31(40)	0
971.38(20)	4830	28(7)	−18(7)
1059.17(20) [f]	2799	−4(15)	0
1184.80(20)	12 867	−66(4)	8(4)
1579.15(30)	(1150)	−60(40)	0
1701.85(25)	5736	−20(3)	0
1739.25(40)	1040	...	...
1763.15(10)	19 098	−28(2)	5(3)
1785.87(P) [g]	(380)	...	...
1946.40(30)	1122	−20(10)	0
2179.10(P) [h]	(3000)	...	...
2244.00(25) [f]	19 102	23(2)	−8(2)
2465.85(30)	3543	−21(6)	0
2645.79(30) [i]	(15 800)	...	...
3162.43(10)	60 450	37(3)	−4(3)

[a] A synthesis of results from ^{14}N + ^{26}Mg, ^{16}O + ^{27}Al, and ^{14}N + ^{27}Al. An entry for A_4 of zero is listed when the inclusion of a term in $P_4(\theta)$ does not improve the fit.

[b] Uncorrected for nuclear recoil. An entry P (for error) means the energy is inferred from known level separations. A square bracket denotes an uncertain assignment to ^{35}Cl.

[c] From ^{14}N + ^{27}Al at $E(^{14}\mathrm{N}) = 40$ MeV. The numbers in parentheses were estimated from known branching ratios or from the $\gamma\gamma$-coincidence data.

[d] Doublet with the ^{36}Cl 2469 → 1951, 517.10(10)-keV γ ray.

[e] Unresolved from the weaker ^{37}Ar 6474 → 5793, 680.34(20)-keV γ ray.

[f] Partially Doppler shifted in the angular distribution spectra.

[g] Inferred from the presence of 680-971 coincidences: not otherwise observed.

[h] Observed in the $\gamma\gamma$ coincidences only.

[i] Doublet with the ^{38}K 2646 → 0, 2646.41(70)-keV γ ray.

for ^{35,36,37}Cl and ^{37}Ar. These results were obtained from a variety of projectile-target combinations at projectile energies in the range 20–60 MeV. A full list of those surveyed is given in Table I.[1-3] The final nuclei under study were observed in all these projectile-target combinations for which $x + y + z \le 3$ (with $z \le 2$), and in some others as well as indicated in Table II. A brief report of the results for ^{37}Cl has already been given.[4]

Extensive and detailed studies of high-spin states in all four nuclei have been reported via the ^{32}S$(\alpha, p)^{35}$Cl reaction,[5,6] the ^{33}S$(\alpha, p)^{36}$Cl reaction,[7] the ^{34}S$(\alpha, p)^{37}$Cl reaction,[8,9] and the ^{34}S$(\alpha, n)^{27}$Ar reaction.[10,11] Thus, in this report heavy emphasis is placed on the new information obtained and the

TABLE IV. Summary of $\gamma\gamma$-coincidence data from the $^{27}Al(^{14}N, np\alpha)^{35}Cl$ reaction. The intensities of coincident γ-ray pairs are indicated as being relatively strong (S), average (M), or weak (W): parentheses enclose cases where the observation is so weak as to be uncertain. An X indicates the coincidence was unobserved, even though from the decay scheme it should be expected.

E_γ (keV)	517	680	882	971	1059	1185	1579	1702	1763	1786	1946	2244	2466	2646	3162
517	···	M	W	M	W	M	(W)		W	X	W	M	S	S	
680	M	···	(W)	W	S	M		W	(W)	(W)	···	S	W	W	S
882	W	(W)	···	(W)	W	(W)	X	W	S	X	X	W	X		
971	M	W	(W)	···	W	M	M	W	W	(W)	S	S	S	M	S
1059	W	S	W	W	···	S		M	X	X			W	M	W
1185	M	M	(W)	M	S	···	M		X	X	S		W	M	S
1579	(W)		X	M		M	···	M	X		S			M	W
1702		W	W	W	M		M	···	X	X	(W)		X	S	
1763	W	(W)	S	W	X	X	X	X	···	X	X	X	X		
1786	X	(W)	X	(W)	X	X		X	X	···		(W)		X	(W)
1946	W		X	S		S	S	(W)	X		···			W	M
2244	M	S	W	S					X	(W)		···	S	S	S
2466	M		X	S	W	W		X	X			S	···	M	S
2646	S	W		M	M	M	M	S		X	W	S	M	···	
3162		S		S	W	S	W			(W)	M	S	S		···

systematics revealed.

The present results are a part of a general program for the nuclear spectroscopy of high-spin states in light nuclei. The experimental procedures and the methods of assigning spins, parities, and γ-ray multipolarities have been described extensively in previous reports[1,2,12-14] and will only be briefly mentioned here. The experimental results are presented in Sec. II and discussed in Sec. III.

II. RESULTS

The bulk of the results will be presented in tabular form. For each of the nuclei $^{35,36,37}Cl$ and ^{37}Ar we present two tables: (1) γ-ray energies,

TABLE V. Energy levels of ^{35}Cl deduced from fusion-evaporation reactions and compared to previous results.

Energy level[a] (keV)	E_γ (keV)	γ-ray decay Branching ratio b	c	d	Mean lifetime (ps) b	c	d
1763.20(10)	1763	100		100			0.46 ± 0.05
2645.31(14)	882			9 ± 1			0.25 ± 0.03
	2645			91 ± 1			
3162.58(10)	517			8 ± 1	41.8 ± 1.8	41.7 ± 1.7[e]	42 ± 3[f]
	3162			90 ± 1			
3942.30(70)[d]	1297			10[g]			0.35 ± 0.045
	2179			90[g]			
4347.32(18)	1185	69 ± 5	64 ± 2	69 ± 3			2.9 ± 1.1
	1702	31 ± 5	36 ± 2	31 ± 3			
5406.58(20)	1059	13 ± 4	9 ± 2			0.40 ± 0.10	
	2244	87 ± 4	91 ± 2				
5926.51(37)	1579	100		100[g]			
6086.91(25)	680	···	85 ± 5		7.7 ± 1.4	9.3 ± 0.8	
	1739	···	15 ± 5				
7872.68(28)	1786	8 ± 5			$0.5 < \tau < 50$		
	1946	22 ± 5					
	2466	70 ± 5					
8844.07(35)	971	100			8 ± 2		

[a] Deduced from the γ-ray energies of Table III.
[b] Present results
[c] Reference 6.
[d] Reference 15.
[e] Reference 16.
[f] Reference 17.
[g] Reference 5.

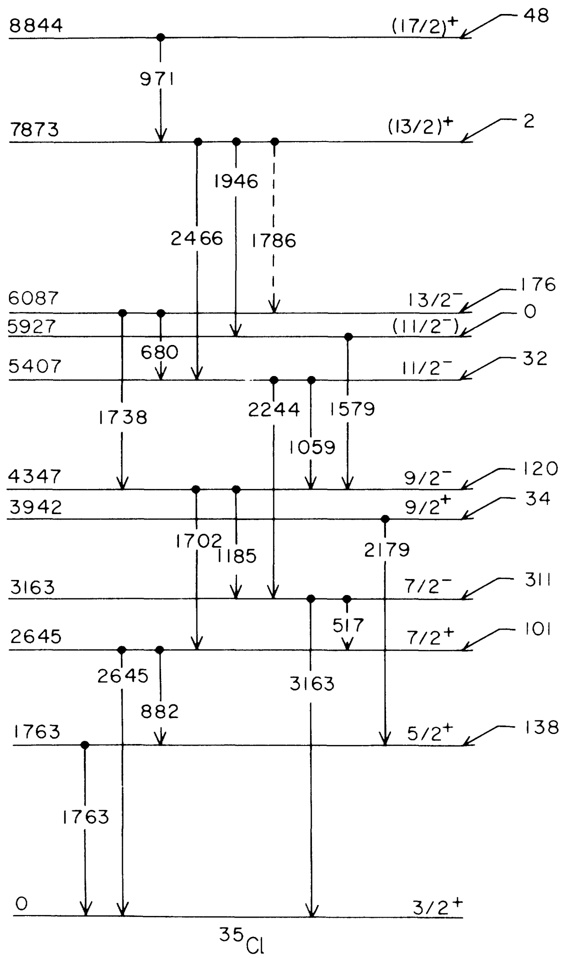

FIG. 1. ^{35}Cl energy levels and γ-ray transitions observed in the fusion-evaporation reactions of Table II. Level and γ-ray energies are in keV. The relative feeding intensities of the levels in the ^{27}Al(^{14}N, $np\alpha$)^{35}Cl reaction at E(^{14}N) =40 MeV are given on the far right. The spin-parity assignments for $E_x < 7$ MeV are from Refs. 5 and 6. The assignments for the top two levels are discussed in the text.

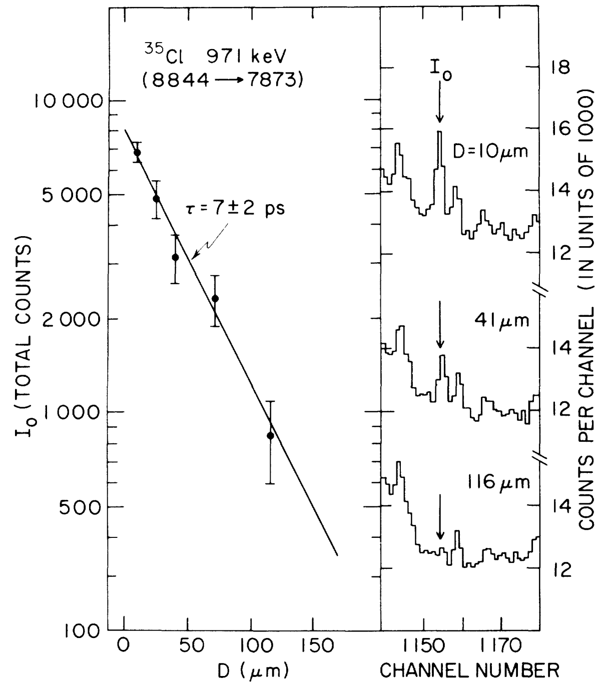

FIG. 2. RDM lifetime results for the ^{35}Cl 971-keV, 8844→ 7873 transition. On the left is shown the decay of the intensity of the stopped component I_0 of the 971-keV transition with the target-stopper distance D. To first order $D = vt$ where v is the recoil ion velocity, and thus I_0 decays as $\exp(-D/v\tau)$ where τ is the mean life associated with the decay. The least-squares fit given by the solid curve was (to first order) to $A\exp(-D/v\tau)+B$. The data which yielded the intensity versus D curve are illustrated on the right.

relative intensities, angular distribution coefficients, and linear-polarization and multipole-mixing-ratio information (if available) and (2) the level energies, branching ratios, and lifetimes. For ^{35,36}Cl we also summarize the $\gamma\gamma$- coincidence data in matrix form. For each nucleus a level scheme is presented summarizing the γ-ray transitions observed in the present results and the final spin-parity assignments. Other figures are given to illustrate the data. We now consider the four nuclei in turn.

^{35}Cl

γ-ray transitions identified as belonging in ^{35}Cl are listed in Table III. The most definitive $\gamma\gamma$-coincidence results used to identify these transitions and place them in a decay scheme come from the ^{27}Al(^{14}N,$np\alpha$)^{35}Cl reaction at E(^{14}N)= 40 MeV. The coincidence matrix summarizing these results is given in Table IV. This matrix and the γ-ray relative intensity, angular distribution, and energy information summarized in Table III lead to the energy level scheme of Fig. 1. Our best values for the level energies are given in Table V together with a comparison of our branching ratio and lifetime information with previous results.[5,6,15-17] The spin-parity assignments of Fig. 1 for the levels below 7 MeV excitation are those determined or quoted by Alenius and Wallander[5] and Lornie *et al.*[6] Our information pertaining to the spin-parity assignments up to and including the 6087-keV level of ^{35}Cl is in agreement with but much less definitive than those previous ^{32}S(α,$p\gamma$)^{35}C results.

Nann *et al.*[18] observed ^{35}Cl levels at 7.87 ± 0.30 and 8.84 ± 0.30 MeV in the ^{33}S(α,d)^{35}Cl reaction with definite $L = 6$ (i.e., $J^\pi = \frac{11}{2}^+ - \frac{17}{2}^+$) angular distribution patterns. We associate these two levels

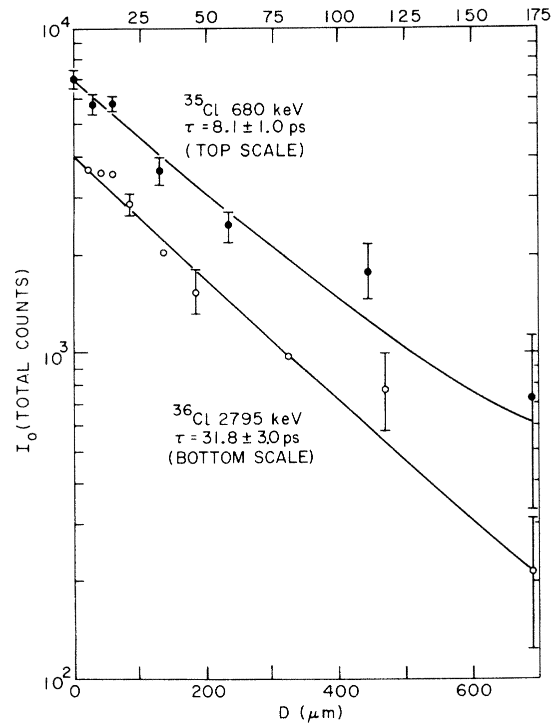

FIG. 3. RDM results for the ^{35}Cl 680-keV 6087→ 5407 and ^{36}Cl 2795-keV 5313→ 2518 transitions. For details see the caption of Fig. 2.

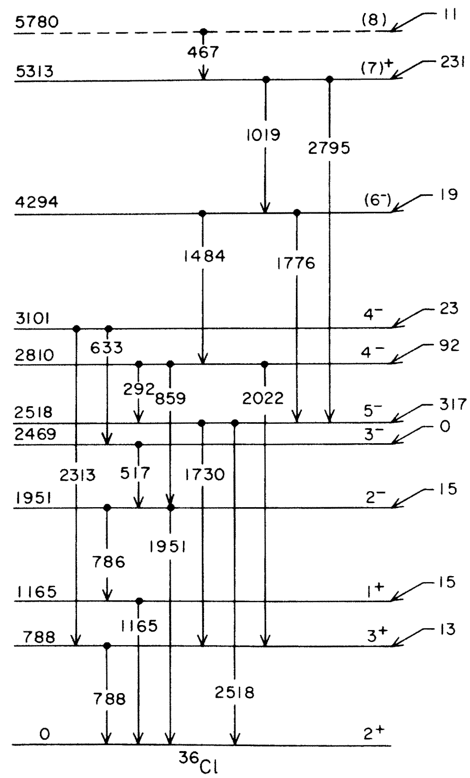

FIG. 4. ^{36}Cl energy levels and γ-ray transitions observed in the fusion-evaporation reactions of Table II. Level and γ-ray energies are in keV. The relative feeding intensities of the levels in the ^{27}Al(^{14}N, $p\alpha$)^{36}Cl reaction at E(^{14}N) =40 MeV are given on the far right. The spin-parity assignments for E_x < 4 MeV are from Refs. 7 and 19 while those for the top three levels are discussed in the text.

with the upper two of Fig. 1; hence, the even-parity assignments to these two levels. The γ-ray transitions deexciting these two levels were previously unobserved.

The most probable spin assignments of $\frac{13}{2}$ and $\frac{17}{2}$ to the ^{35}Cl 7873- and 8844-keV levels are based on the γ-ray angular distributions and the relative strengths of the direct feeding of the levels. That is, we have invoked the usual but well-established criteria for obtaining spin-parity assignments in fusion-evaporation reactions.[1,2,19,20]

From Table III we see that the two measured angular distributions for the decay to $J^\pi = \frac{11}{2}^-$ states from the 7873-keV level are both characteristic of pure dipole $J \to J \mp 1$ transitions while the 971-keV 8844→ 7873 transition has a characteristic pure quadrupole $J \to J \mp 2$ pattern.[20] Also the relatively strong formation of the 8844-keV level strongly suggests it is an yrast level, i.e., $J > \frac{13}{2}$. These data jointly favor spin assignments of $\frac{13}{2}$ for the 7875-keV level and $\frac{17}{2}$ for the 8844-keV level.

The branching ratios obtained in the present work are in agreement with the previously quoted results.

The lifetime information was obtained mainly from the recoil distance method (RDM).[21] However, in some cases, (e.g., the ^{35}Cl 7873-keV level) lower limits were obtained from the absence of any discernible Doppler shifts[21] in the γ-ray singles spectra. The lifetime information for ^{35}Cl and ^{36}Cl was obtained from ^{14}N+ ^{27}Al and ^{14}N + ^{24,26}Mg. The quoted lifetime for the 8844-keV level is an average of values of 7 ± 2 and 11 ± 5 ps from ^{14}N+ ^{26}Mg and ^{14}N+ ^{27}Al, respectively. The results from ^{14}N+ ^{26}Mg are illustrated in Fig. 2. The quoted lifetime of 7.7 ± 1.4 ps for the ^{35}Cl 6087-keV level is an average of four determinations (one of which is illustrated in Fig. 3): the four determinations comprise results on the 680- and 2244-keV γ rays from the 6087 → 5407 and 6087 → 5407 → 3163 transitions observed in the ^{14}N+^{27}Al and ^{14}N+ ^{24}Mg reactions. Since the 5407-keV level has a lifetime short compared to that of the 6087-keV level,[6] the 680- and 2244-keV γ rays decay with a time characteristic of the 6087-keV level with a small effect (taken into account) due to feeding from the 7873- and 8844-keV levels.

TABLE VI. ^{36}Cl γ rays observed in fusion-evaporation reactions.

γ-ray energy [c] (keV)	Relative [d] intensity	Angular [a] distribution (%) A_2	A_4	Linear [b] polarization (%) Exp.	Predicted
292.13(10) [e]	(4060)	...	...		
466.57(15)	1145	−19(11)	0		
517.10(10) [f]	(1300)	...	...		
632.50(30)	1261	−21(10)	0		
[756.90(30)] [g]	(1430)	...	...		
786.04(50) [h]	(1430)	...	...		
788.44(10)	63 919	29(2)	−3(3)	−28(5)	−28(5), $\delta=-1.1\pm0.3$
859.41(30)	1322	16(9)	0		
1019.01(10)	14 616	−25(3)	0	+31(26)	+33(5), $\delta=0$
1164.94(20)	2868	−17(5)	0		
1484.10(50)	1600	21(17)	0		
1729.80(20)	56 320	21(2)	−11(2)	−49(11)	−49(11), $\delta=+0.19\pm0.10$
1776.06(10) [i]	14 996	57(11)	0		
1951.08(20)	2774	22(10)	0		
2022.15(20)	5313	−25(5)	0	+55(33)	+33(7), $\delta=0$
2312.14(50)	961	...	...		
2518.30(30)	3751	52(7)	−9(8)	+90(90)	+102(20), $\delta=0$
2795.05(30)	9468	37(5)	−13(5)	−150(100)	−62(12), $\delta=0$
[3842.19(100)] [j]	<1000	...	...		

[a] An entry for A_4 of zero (with no error) is listed when the inclusion of a term in $P_4(\theta)$ does not improve the fit.

[b] The experimental results are from the ^{18}O+^{24}Mg results of Ref. 2. The predictions are for the spin-parity values of Fig. 4 and the indicated angular distributions and multipole-mixing ratios. For the 788- and 1730-keV transitions, the multipole-mixing ratio δ is derived from a comparison of the Exp. and Predicted polarizations. For the other transitions the indicated value of δ is *assumed* in calculating the predicted polarization.

[c] Uncorrected for nuclear recoil. The number in parentheses is the uncertainty in the last place. A square bracket denotes an uncertain assignment to ^{36}Cl.

[d] From the ^{27}Al(^{14}N,$p\alpha$)^{36}Cl reaction at 40 MeV. The numbers in parentheses were estimated and/or obtained from other reactions.

[e] Obscured by the ^{173}W 291.719(8)-keV γ ray in the angular distribution studies.

[f] Doublet with the ^{35}Cl 3163 → 2646, 517.26(10)-keV line.

[g] Seen in ^{12,13}C+^{26}Mg singles and possibly in ^{14}N+^{27}Al coincidences.

[h] Not resolved from the much more intense 788.44-keV line.

[i] Poorly resolved from the ^{28}Si 1779 → 0, 1778.81(9)-keV γ ray.

[j] Possibly seen in ^{14}N+^{27}Al coincidences and ^{13}C+^{26}Mg singles.

^{36}Cl

γ-ray transitions identified as belonging in ^{36}Cl are listed in Table VI and the $\gamma\gamma$- coincidence matrix from the ^{27}Al(^{14}N,$p\alpha$)^{36}Cl reaction at $E(^{14}\mathrm{N})$ = 40 MeV is given in Table VII. The energy levels are listed in Table VIII where our branching ratio and lifetime results are compared to previous results[7,15,16,22] and the level scheme shown in Fig. 4. The levels below 4 MeV were well studied previously and our results for these levels add very little that is new. The 4294- and 5313-keV levels were also observed by Rascher *et al.*[16] via fusion-evaporation reactions, and the 5313-keV level by Sherr, Kouzes, and Del Vecchio[23] via the ^{34}S(α, d)^{36}Cl reaction. The 467-keV γ ray is definitely identified with ^{36}Cl but its placement in the decay scheme is not definite—hence the dashed line for the 5780-keV level.

The spin-parity assignments for the upper three levels are based on the angular distribution and linear polarization data of Table VI and the relative direct feeding intensities shown in Fig. 4. The angular distribution of the 2795-keV γ ray is characteristic of a $J \to J\mp2$ quadrupole transition and the strong direct feeding of the 5313-keV level indicates an yrast level; hence $J=7$. The linear polarization has a large uncertainty but favors $M2$ (over $E2$ which would have the opposite sign) in agreement with the even-parity assignment from the (α,d) results of Sherr *et al.*[23]

The feeding suggests that the 5780-keV level is

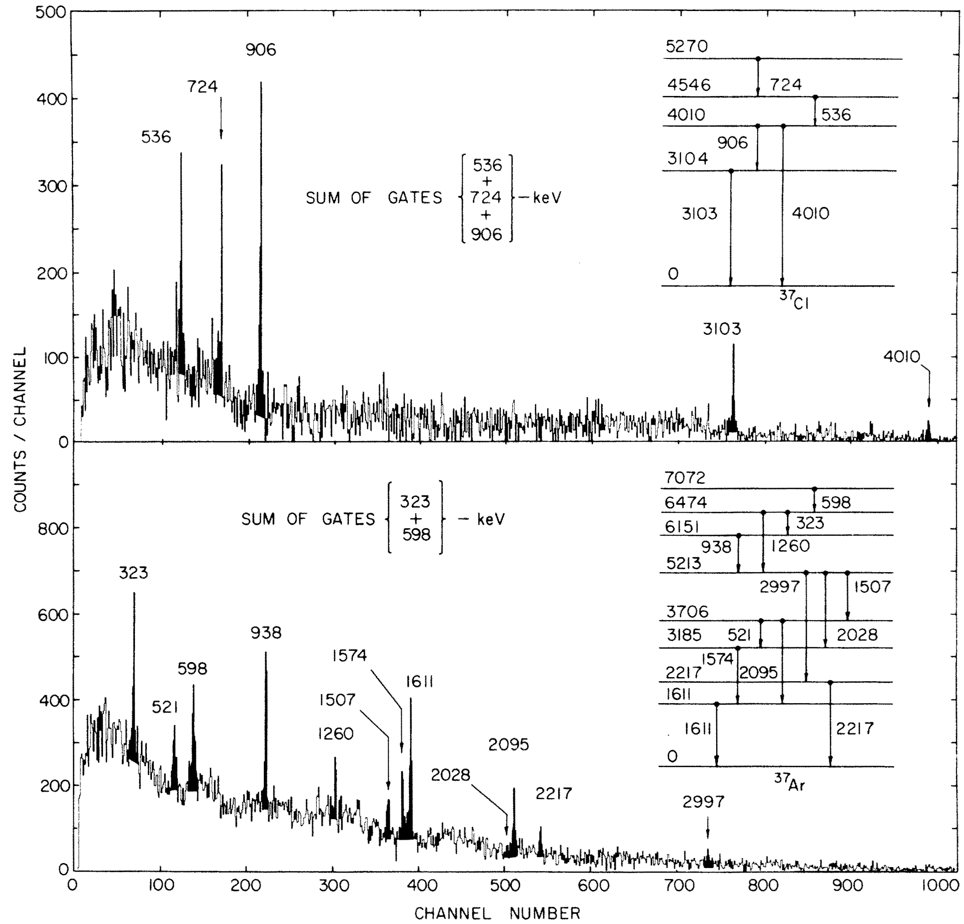

FIG. 5. Typical $\gamma\gamma$-coincidence results for ^{37}Cl and ^{37}Ar from ^{26}Mg + ^{14}N at $E(^{14}N) = 40$ MeV. Energies are in keV. The inserts indicate the placement of the γ-ray transitions in the decay schemes.

TABLE VII. Summary of $\gamma\gamma$-coincidence data from the $^{27}Al(^{14}N, p\alpha)^{36}Cl$ reaction. The intensities of coincident γ-ray pairs are indicated as being relatively strong (S), average (M), or weak (W): parentheses enclose cases where the observation is so weak as to be uncertain. An X indicates the coincidence was unobserved, even though from the decay scheme it should be expected.

E_γ (keV)	292	467	517	633	788 [a]	859	1019	1165	1484	1730	1776	1951	2022	2312	2795
Gate															
292	···	(W)			S		W		M	S					
467	X	···			S					S					
517			···	M	W			W				M			
788 [a]	M	W	W	(W)	(W)	(W)	S	W	(W)	S	S		M	X	S
1019	W	(W)		W	S	X	···		(W)	S	S		(W)		
1730	M	W			S		S		(W)	···	S				S
1776		X			S		S			S	···				
1951															
2022		X			S		(W)		(W)						
2795		X			S					S					

[a] Assumed doublet of 786.04 and 788.44 keV.

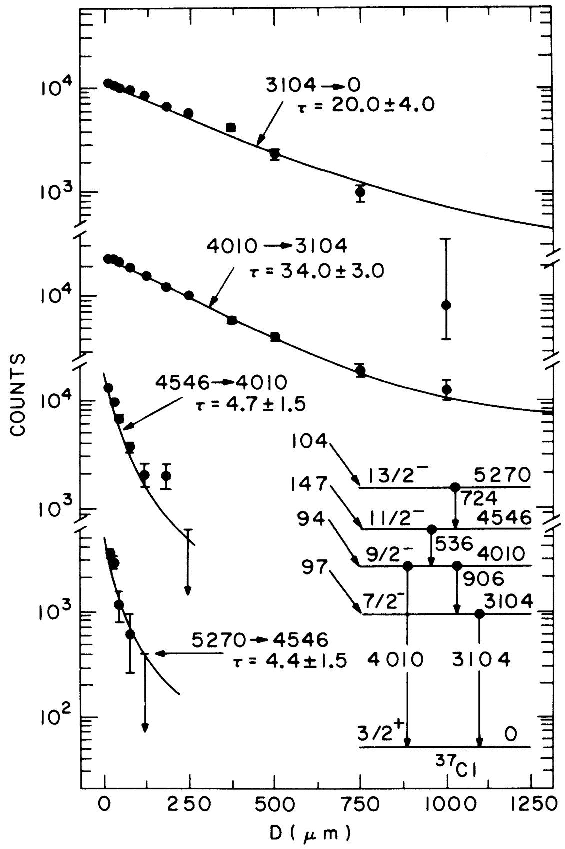

FIG. 6. ^{37}Cl energy levels and RDM results. The energy level diagram indicates the levels and γ-ray transitions observed in the fusion-evaporation reactions of Table II. Levels and γ-ray energies are in keV. The relative feeding intensities of the levels in the ^{26}Mg(^{14}N, $n2p$)^{37}Cl reaction at E(^{14}N) = 40 MeV are given on the left. The spin-parity assignments are from Ref. 9. The RDM results were obtained using the branching ratios of Table X and the feeding intensities shown above. The fits were to the generalization of $\exp(-D/v\tau)$ to include the dependence on several different lifetimes.

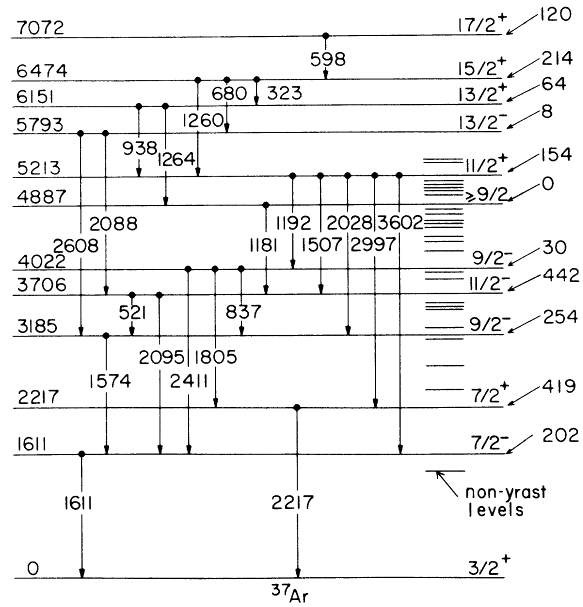

FIG. 7. ^{37}Ar energy levels and γ-ray transitions observed in the fusion-evaporation reactions of Table II. Levels and γ-ray energies are in keV. The relative feeding intensities of the levels in the ^{26}Mg(^{14}N, $2np$)^{37}Ar reaction E(^{14}N) = 40 MeV are given at the far right. The spin-parity assignments are from Ref. 11. The selectivity of the fusion-evaporation reaction is illustrated by showing the known non-yrast levels for $E_x < 5.4$ MeV on the right. No decays from any of these levels were observed in the present work.

an yrast level and the angular distribution of the 467-keV γ ray indicates a $J \to J \mp 1$ dipole transition; hence $J = 8$ for the 5780-keV level. The 1019-keV γ transition has an angular distribution and linear polarization characteristic of a $J \to J \mp 1$ $E1$ transition; hence $J^\pi = 6^-$ is suggested for the 4294-keV level. The fact that these assignments, although highly favored, are nonrigorous is indicated by parentheses in Fig. 4. We note that with these assignments the 1484-keV transition from the 4294-keV level to the 4^- 2810-keV level is $E2$ while the 1776-keV transition from the 4294-keV level to the 5^- 2518-keV level is, from its angular distribution, an $E2/M1$ mixture (with $\delta \simeq -0.6$). However, if the 4294-keV level had even parity these transitions would be $M2$ and $M2/E1$ and in view of the 10-ps upper limit to the lifetime (see Table VIII) this seems highly unlikely.

The ^{36}Cl branching ratio and lifetime information obtained in this work is in fair agreement with previous information. The RDM data yielding the lifetime of the 5313-keV level are illustrated in Fig. 3.

^{37}Cl

The γ rays assigned to ^{37}Cl are listed in Table IX. The best data were obtained from ^{14}N + ^{26}Mg and definite identification with ^{37}Cl was made with the aid of ^{14}N + ^{26}Mg $\gamma\gamma$-coincidence data taken at E(^{14}N) = 40 MeV. An example of the information obtained from this data is illustrated in Fig. 5.

Unlike ^{35,36}Cl, no γ-ray transitions were observed in addition to those reported in the (α,p) work.[8,9] The spin-parity assignments of Fig. 6 follow the ^{34}S(α,p)^{37}Cl results of Nolan *et al.*[9]; our results are consistent with these previous ones but less definitive. The agreement of our conclusions with the previous (α,p) results of Nolan *et al.*[7] is best illustrated by the comparison given in Table IX of the multipole-mixing ratios and in

TABLE VIII. Energy levels of ^{36}Cl deduced from fusion-evaporation reactions.

Energy level [a] (keV)	E_γ (keV)	γ-ray decay Branching ratio a	b	c	Mean lifetime (ps) a	d	b
788.45(10)	788		100	100		23 ± 2	30 ± 1
1164.96(20)	1165		100	100		10.4 ± 0.5	7.1 ± 0.5
1951.14(20)	786		34 ± 8 [d]			2.95 ± 0.14	2.3 ± 0.2
	1951		66 ± 8 [d]				
2468.18(22)	517		100	91			<1
2518.30(18)	1730	94 ± 1	95.6 ± 0.5	93		2300 ± 160 [e]	2360 ± 160
	2518	6 ± 1	4.4 ± 0.5	7			
2810.54(14)	292	38 ± 4	39 ± 1			4.9 ± 1.0	3.3 ± 0.3
	859	12 ± 4	10 ± 2				
	2022	50 ± 4	51 ± 1				
3100.68(37)	633	57 ± 20		62		0.20 ± 0.05 [c]	
	2313	43 ± 20		38			
4294.41(21)	1484	9 ± 2			<10	<20 [e]	
	1776	91 ± 2					
5313.44(23)	1019	61 ± 3	53 ± 4 [e]		32 ± 3	27.2 ± 1.7 [e]	
	2795	39 ± 3	47 ± 4 [e]				
[5780.01(25)]	467	100			$0.5 < \tau < 1000$		

[a] Present results.
[b] Reference 7.
[c] Reference 15.
[d] Reference 9.
[e] Reference 16.

Table X of the branching ratios extracted from the two experiments. The agreement is excellent.

The ^{37}Cl lifetimes determined in the present experiment were obtained as averages of the results from RDM measurements in the ^{18}O + ^{24}Mg and ^{14}N + ^{26}Mg reactions. Data from the latter are shown in Fig. 6. The results are given in Table X for comparison to other measurements.[9,17] As can be seen, the agreement between the present experiment and Nolan *et al.*[9] is excellent for the 4010-keV level, and at least fair for the 5270- and 4446-keV levels. For the 3104-keV level our result of $\tau = 22.0 \pm 4.0$ ps is in good agreement with the value measured by Brandolini *et al.*[17] ($\tau = 27 \pm 4$ ps), while both measurements are in serious disagreement with the value $\tau = 48 \pm 5$ ps given by Nolan *et al.*[9] In the absence of any further information, it appears that the net data on the ^{37}Cl 3104-keV level favor the shorter lifetime.

^{37}Ar

The ^{37}Ar γ rays are listed in Table XI and the derived energy levels in Table XII. As was the

TABLE IX. ^{37}Cl γ rays observed in fusion-evaporation reactions.

γ-ray energy [b] (keV)	Relative [c] intensity	Angular distribution [a] (%) A_2	A_4	Linear polarization [a] (%)	Multipole-mixing ratio d	e
535.91(10)	25 071	−26(4)	8(4)	−26(7)	+0.02(2)	−0.04(2)
724.44(15)	10 397	−22(6)	17(8)	−44(15)	−0.12(4)	−0.07(4)
906.33(10)	24 252	30(3)	8(4)	−66(16)	−0.54(6)	−0.73(4)
3103.40(20)	33 926	29(7)	8(9)	+9(51)	−0.16(3)	−0.18(1) [f]
4009.65(*P*)	10 255	37(10)	7(10)	···	0.0(1)	0.00(2)

[a] From ^{18}O + ^{24}Mg at $E(^{18}\text{O}) = 40$ MeV (Ref. 2). Although linear-polarization data were also obtained from ^{14}N + ^{26}Mg (Ref. 2) those for ^{18}O + ^{24}Mg were more accurate and are considered more reliable.
[b] Uncorrected for nuclear recoil. An entry *P* (for error) means the energy is inferred from known level separations.
[c] From ^{14}N + ^{26}Mg at $E(^{14}\text{N}) = 40$ MeV.
[d] Present results from a simultaneous consideration of the angular distribution and linear-polarization results assuming the spin-parity assignments of Fig. 5 and the lowest and next to lowest allowed multipoles only. Data from both the ^{18}O + ^{24}Mg and ^{14}N + ^{26}Mg reactions have been used.
[e] Reference 9.
[f] Reference 15.

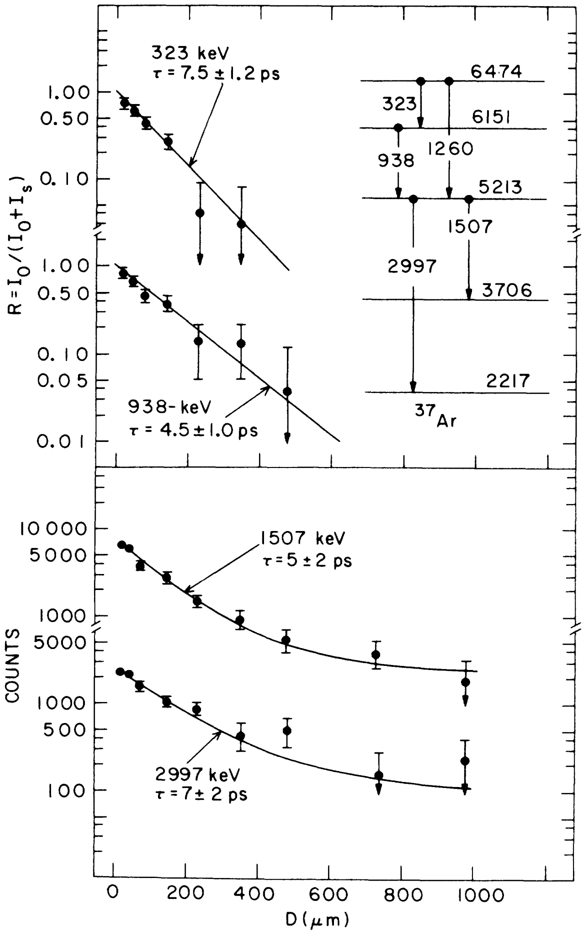

FIG. 8. ^{26}Mg + ^{14}N RDM results for ^{37}Ar. For details see the captions of Figs. 2 and 6.

case for ^{37}Cl, the best data were obtained from ^{14}N + ^{26}Mg and the ^{37}Ar decay scheme was constructed mainly from the ^{14}N + ^{26}Mg $\gamma\gamma$-coincidence data as exemplified in Fig. 5. The decay scheme in Fig. 7 includes only those γ rays observed in the present work. As in the case of ^{37}Cl, all the γ rays of Table XI and energy levels of Fig. 7 were previously observed in ^{34}S + α.[10,11] The spin-parity assignments of Fig. 7 are those of Gadeken *et al.*[11] Our results are consistent with these assignments but less definitive.

As is shown by a comparison of the last two columns of Table XI, the multipole-mixing ratios extracted from our angular distribution data are consistent with those obtained by Gadeken *et al.*[11] The branching ratios listed in Table XII are also in fair agreement with those of Ref. 11. Our RDM results are illustrated in Fig. 8. The lifetimes obtained for the 6473- and 6151-keV levels are in excellent agreement with the ^{34}S(α,n)^{37}Ar results,[11] while for the 5213-keV level the agreement is within 1.2 standard deviations.

III. DISCUSSION

In this section we consider two topics. First, we shall discuss briefly the new results obtained in this work, and, second, we consider some aspects of the systematics of yrast levels in the region $35 \le A \le 43$ and the formation of these states by fusion-evaporation reactions. For both topics it is helpful to have as a basis for discussion weak-coupling calculations for the excitation energies of the yrast levels of ^{35,36,37}Cl and ^{37}Ar.

We use the weak-coupling model of Bansal and French[24] as discussed and applied by Bernstein[25] and more recently by Sherr, Kouzes, and Del Vecchio[23] and by Sherr and Bertsch.[26] As applied to the $d_{3/2}^{-m}f_{7/2}^{n}$ configurations under consideration here,[27] the model predicts the excitation energies of the multiplets formed by coupling the states of $d_{3/2}^{-m}$ with angular momenta $\vec{J}_h$ to those of $f_{7/2}^{n}$ with angular momenta $\vec{J}_p$, i.e., the multiplets formed from $\vec{J}_p + \vec{J}_h$. No residual interaction is introduced to split these multiplets so that the predicted excitation energy is taken to correspond

TABLE X. Energy levels of ^{37}Cl deduced from fusion-evaporation reactions and compared to previous results.

Energy level [a] (keV)	E_γ (keV)	γ-ray decay Branching ratio a	b	Mean lifetime (ps) a	b	c
3103.54(20)	3103	100	100	22.0 ± 4.0	48 ± 5	27 ± 4
4009.88(22)	906	69 ± 2	69 ± 1	34.0 ± 2.0	31 ± 3	
	4010	31 ± 2	31 ± 1			
4545.79(24)	536	100	100	4.7 ± 1.2	2.7 ± 0.6	
5270.24(29)	724	100	100	4.4 ± 1.5	2.7 ± 0.4	

[a] Present results.
[b] Reference 9.
[c] Reference 17.

TABLE XI. ^{37}Ar γ rays observed in fusion-evaporation reactions.

γ-ray energy [a] (keV)	Relative [b] intensity	Angular distribution [c] A_2 (%)	A_4 (%)	Linear polarization [c] P (%)	Multipole-mixing ratio d	e
322.80(12)	22 295	−36(3)	+1(4)	−20(10)	+0.10(3)	+0.05(2)
521.12(25)	13 641	−25(10)	0	···	−0.03(10)	−0.11(7)
597.92(15)	11 992	−29(8)	+10(10)	−22(14)	+0.03(3)	−0.01(1)
680.34(20) [f]	(9497)	···	···	···	···	+0.03(3)
836.90(40)	2607	···	···	···	···	+0.02(7)
937.55(20) [g]	(19 572)	−17(5)	+11(5)	−43(15)	−0.14(3)	−0.10(1)
1180.90(70)	3457	···	···	···	···	···
1191.50(30)	4270	−5(3)	0	···	−0.11(5)	−0.14(2)
1260.45(30)	1583	+36(12)	0	···	+0.04(3)	···
1263.80(26)	9095	···	···	···	···	···
1506.98(20)	14 650	+32(4)	+9(4)	···	+0.09(6)	+0.08(4)
1573.68(20)	55 153	+32(4)	+7(5)	−54(20)	−0.49(8)	−0.64(5)
1611.24(9) [h]	130 551	+14(2)	−3(2)	−14(6)	+0.14(5)	+0.12(2)
1805.41(40)	4262	···	···	···	···	+0.00(2)
2028.26(40)	7300	···	···	···	···	+0.08(2)
2087.80(50) [i]	4038	···	···	···	···	···
2094.90(30)	52 642	+24(13)	−4(3)	+47(28)	+0.02(3)	+0.04(4)
2216.80(20)	54 304	+26(3)	−2(14)	−72(74)	+0.03(5)	+0.00(2)
2411.18(60)	444	···	···	···	···	−1.9(4)
2608.15(35) [i]	6221	+6(16)	0	···	+0.05(5)	−0.01(3)
2996.52(50)	8161	+35(6)	+6(6)	···	−0.08(8)	−0.02(2)
3602.20(50)	2141	···	···	···	···	−0.16(9)

[a] Uncorrected for nuclear recoil.
[b] From $^{14}N+^{26}Mg$ at $E(^{14}N)=40$ MeV. The numbers in parentheses have been corrected for unresolved contaminants, using information on branching ratios and intensities obtained from other data.
[c] An average of all reactions studied.
[d] Present results from a simultaneous consideration of the angular distribution and linear-polarization results assuming the spin-parity assignments of Fig. 6 and the lowest and next to lowest multipoles only.
[e] Reference 15 for $E_x<3$ MeV and Ref. 11 for $E_x>3$ MeV.
[f] Unresolved from the ^{35}Cl 6087→5407, 680.22(15)-keV γ ray. The energy is from $^{13}C+^{26}Mg$ at $E(^{13}C)=20$–25 MeV.
[g] Unresolved from ^{18}F 937→0, 937.21(12)-keV γ ray from transfer and contaminant (^{12}C, ^{16}O targets) reactions.
[h] Unresolved from the ^{25}Mg 1612→0, 1611.63(13)-keV γ ray from transfer and contaminant reactions.
[i] Intensities quoted for the 5793-keV level may be too low, by as much as a factor of 2, because a possible Doppler-broadened component could not be reliably extracted by the line shape analysis.

to the centroid of the multiplet or, more usually, to it's maximal-spin member. We have recently discussed the comparison of the weak-coupling model to the yrast spectra of ^{38}Ar[14] and ^{39}Ar.[28] In these two cases the root-mean-square (rms) difference between the predictions and experiment for yrast states of maximal spin is approximately 400 keV which is as good as current large-basis shell-model predictions.

The weak-coupling predictions for the yrast levels of ^{35,36,37}Cl and ^{37}Ar are shown in Fig. 9 together with the experimental yrast levels. In all cases, the $d_{3/2}^{-m}$ states are well-known experimentally[15] and described adequately by shell-model calculations. The $f_{7/2}$ states involved are the ^{41}Ca-^{41}Sc $J=\frac{7}{2}$ ground states, while the $f_{7/2}{}^2$ states are the yrast 0^+, 2^+, 4^+, and 6^+ states of ^{42}Ca and the low-lying $J^\pi=0^+$, $T=1$ and $J^\pi=7^+$, $T=0$ states of ^{42}Sc.[15] Inspection of Fig. 9 leads one to the conclusion that all the high-spin ($J\geq 5$) yrast levels of ^{35,36,37}Cl and ^{37}Ar can probably be accounted for by configurations generated by promoting one or two nucleons from the (s,d) shell to the (f,p) shell. We shall return to this observation below, but now we consider the incorporation of the present results into local systematics.

In ^{36}Cl our data suggested but did not establish a level at 5.78 MeV which, if present, is most

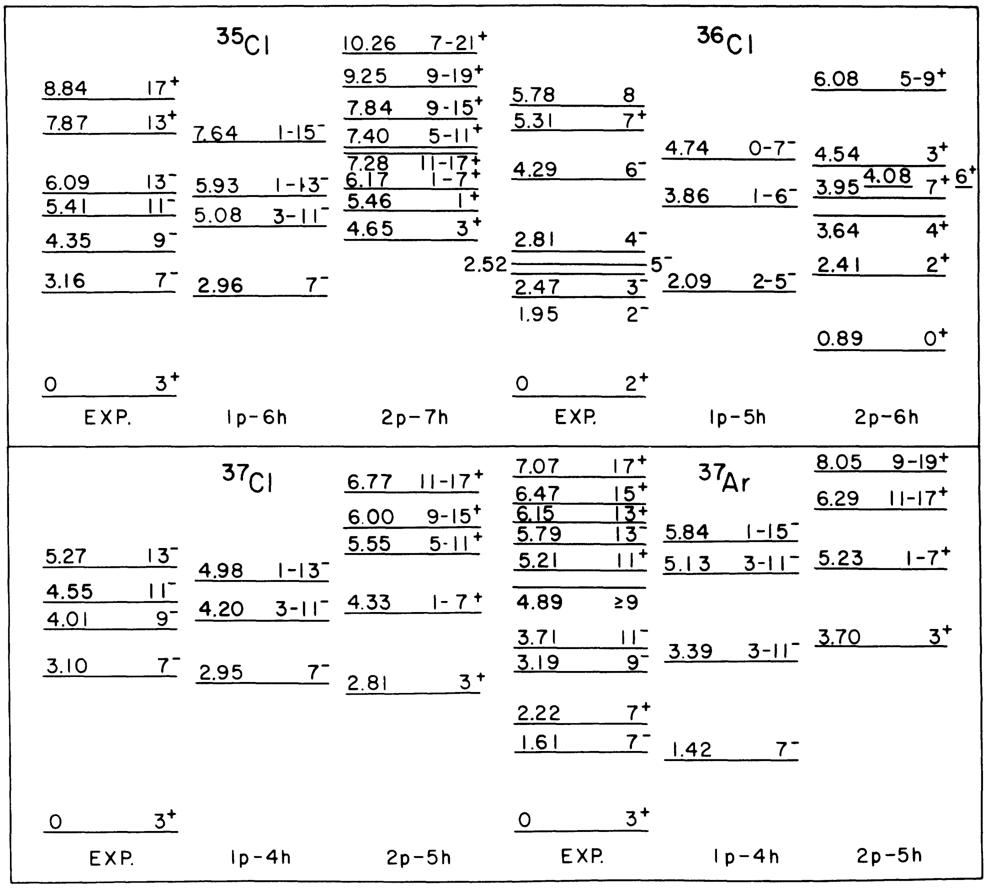

FIG. 9. Comparison of the high-spin spectra of ^{35,36,37}Cl and ^{37}Ar to the predictions of weak-coupling calculations. Energies are in MeV. For the odd-A nuclei, $2J$ is shown instead of J. The weak-coupling predictions use the parameters [defined by Bansal and French (Ref. 24)] $a=-0.25$ MeV, $b=2.5$ MeV, $c=-0.5$ MeV.

likely $J=8$. The weak-coupling predictions would then suggest $J^\pi=8^+$ from ^{34}S$(J^\pi=2^+)\otimes^{42}$Sc$(J^\pi=7^+)$.

In ^{35}Cl we observed the γ-ray decay of two levels previously observed only in the ^{33}S$(\alpha,d)^{35}$Cl reaction.[17] The most interesting aspect of the γ decay is that the 971-keV 8844 → 7873 transition between the $\frac{17}{2}^+$ and $\frac{13}{2}^+$ states has a lifetime of 8 ± 2 ps corresponding to a single-particle strength of 17 ± 4 Weisskopf units (W.u.). By contrast, a recent survey[16] of $E2$ transitions between high-spin $d_{3/2}^{-m}f_{7/2}^{\,n}$ states in $37\le A\le 43$ nuclei is remarkable in that 23 of 26 $E2$ transition strengths lie between 0.05 and 7 W.u., with an average value of 3 W.u. Only three transitions have strengths greater than 7 W.u., and two of these are in ^{37}Ar. The explanation of this apparent anomaly would seem to lie in the complexity of the states involved. In ^{35}Cl the $A=33$ nuclei contributing to the states describable as two particles and seven holes (2p-7h) relative to the doubly-closed shell of ^{40}Ca lie near the middle of the (s,d) shell and have a relatively high density of low-lying states which can couple to $(f_{7/2}^{\,2})_{J=6^+7^+}$ to form $\frac{17}{2}^+$ and $\frac{13}{2}^+$ states in ^{35}Cl. Thus, the complexity needed for collective phenomena is present. This complexity is expected to diminish rapidly as the doubly-closed shell at ^{40}Ca is approached. Hence the single-particle nature of the $E2$ transitions for $A\simeq40$ is not unexpected. In other words, where the weak-coupling model works well and generates unequivocal predictions, noncollective $E2$ transitions are expected; where the weak-coupling predictions are ambiguous, collective $E2$ transitions are not surprising. In this regard, note that there are three different weak-coupling multiplets in Fig. 9 which can contribute to the ^{35}Cl 8.84-MeV $\frac{17}{2}^+$ state.

Two interesting conclusions can be deduced from the comparison of weak-coupling predictions and experiment shown in Fig. 9. First, not all the yrast levels from $d_{3/2}^{-m}f_{7/2}$ and $d_{3/2}^{-m}f_{7/2}^{\,2}$ which are energetically available were observed in these reactions and, second, no states were observed

TABLE XII. Energy levels of ^{37}Ar deduced from fusion-evaporation reactions and compared to previous results.

Energy level [a] (keV)	E_γ (keV)	γ-ray decay Branching ratio b	c	d	Mean lifetime (ps) b	e
1611.28(9)	1611	100	100	100		6300 ± 200
2216.87(20)	2217	100	100	100		0.52 ± 0.07
3185.00(22)	1574	100	100	100		0.30 ± 0.04
3706.18(23)	521	18 ± 2	15	14		0.37 ± 0.095
	2095	82 ± 2	85	86		
4021.84(38)	837	36 ± 4	26 ± 2			0.040 ± 0.015
	1805	58 ± 6	68 ± 1			
	2411	6 ± 2	6 ± 2			
4887.10(73)	1181	100	100			
5213.36(24)	1192	12 ± 3	11 ± 2	···	6 ± 2	3.6 ± 0.3
	1507	41 ± 4	41 ± 2	52		
	2028	16 ± 4	19 ± 1	16		
	2997	25 ± 4	20 ± 5	32		
	3602	6 ± 3	9 ± 4	···		
5793.36(39)	2088	60 ± 10	~45			0.125 ± 0.025
	2608	40 ± 10	~55			
6150.92(31)	938	75 ± 5	~75		4.5 ± 1.0	4.6 ± 0.6
	1264	25 ± 5				
6473.72(34)	323	67 ± 5	66 ± 3	60	7.5 ± 1.2	6.3 ± 0.6
	680	28 ± 5	34 ± 3	···		
	1260	5 ± 2	···	40		
7071.64(37)	598	100	100	100		0.55 ± 0.12

[a] Deduced from the γ-ray energies of Table XI.
[b] Present results.
[c] Reference 11.
[d] Reference 10.
[e] Reference 15 for $E_x < 3.5$ MeV, Ref. 10 for $E_x > 3.5$ MeV.

with more complexity than two-nucleon excitations out of the (s,d) shell. Enlarging the discussion to the fusion-evaporation studies of $d_{3/2}^{-m}f_{7/2}$ states of $35 \le A \le 43$ nuclei carried out since 1972, these two statements still stand (except for the 4p-4h states of ^{40}Ca which are, however, excited relatively weakly[29,30]).

As regards the first point, note that in ^{36}Cl the predicted 9^+ level was not observed, in ^{37}Cl none of the even-parity levels have been observed, and in ^{37}Ar the $\frac{19}{2}^+$ level is still unobserved.

As regards the second point, an example would be the ^{36}Cl 3p-7h state formed from the 3123-keV $\frac{19}{2}^-$ state of ^{43}Sc coupled to the $\frac{3}{2}^+$ ground state of ^{33}S. This 8^--11^- multiplet is predicted at an excitation energy of 8.6 MeV and is energetically available to the reactions studied.[31] A more detailed consideration of three- and four-nucleon excitation out of the $(2s,1d)$ shell indicates that numerous yrast levels from configurations more complicated than the ones identified are energetically accessible in these fusion-evaporation reactions in $30 \lesssim A \lesssim 50$ nuclei. A very worthwhile program of study would be a detailed theoretical investigation of the dependence of the (HI,$xn,yp,z\alpha$) cross section on the excitation energy, spin, and *structure* of the levels of the final nucleus. The quite puzzling difference in formation of even-parity 2p-5h states in ^{37}Cl (where none are seen) and ^{37}Ar (where states up to $\frac{17}{2}^+$ are seen) would be a natural part of this study. Although some very successful studies[13,19] of (HI,$zn,yp,z\alpha$) reactions have been carried out using the Hauser-Feshbach form of the statistical model, these studies have not gone into the questions raised here in any detail, but, by and large, have dealt instead with understanding the formation of levels that were observed.

Note added in proof. Additional lifetime measurements have recently been reported for ^{36}Cl and ^{37}Cl which are in agreement with, and thus support, the present results given in Tables VIII and X. These additional results are as follows: ^{36}Cl (1165-keV level), $\tau = 13 \pm 4$ ps;[32] ^{37}Cl (3104-keV level), $\tau = 20 \pm 3$ ps,[32] 16 ± 9 ps,[33] 19.6 ± 3 ps;[34] ^{37}Cl (4010-keV level), $\tau = 34 \pm 4$ ps,[32] 32.8 ± 2.0 ps.[33] In particular, these data clearly support the present result $\tau = 22.0 \pm 4.0$ ps given in Table X for the ^{37}Cl 3104-keV level.

*Work performed under the auspices of the U. S. Energy Research and Development Administration.

†Guest physicist. Permanent address: University of Auckland, Auckland, New Zealand.

[1]E. K. Warburton, J. J. Kolata, J. W. Olness, A. R. Poletti, and Ph. Gorodetzky, At. Data Nucl. Data Tables 14, 147 (1974).

[2]J. W. Olness, A. H. Lumpkin, J. J. Kolata, E. K. Warburton, J. S. Kim, and Y. K. Lee, Phys. Rev. C 11, 110 (1975).

[3]Most of the results for the first 10 projectile-target combinations have been compiled. See Ref. 1 for a list of γ-ray energies, relative intensities, angular distribution coefficients, and excitation function results. Some linear-polarization results are compiled in Ref. 2. A compilation for all 23 projectile-target combinations is available on request to one of the authors (EKW).

[4]J. W. Olness, Ph. Gorodetzky, J. J. Kolata, E. K. Warburton, and A. R. Poletti, Bull. Am. Phys. Soc. 19, 75 (1974).

[5]N. G. Alenius and E. Wallander, Phys. Scr. 8, 129 (1973).

[6]P. R. G. Lornie, E. M. Jayasinghe, G. D. Jones, H. G. Price, M. F. Thomas, P. J. Twin, and P. J. Nolan, J. Phys. A (London) 7, 1977 (1974).

[7]P. J. Nolan, P. A. Butler, P. E. Carr, L. L. Gadeken, A. N. James, J. F. Sharpey-Schafer, and D. A. Viggars, J. Phys. A (London) 6, L37 (1973); P. J. Nolan, A. J. Brown, P. A. Butler, L. L. Green, A. N. James, C. J. Lister, J. D. MacArthur, and J. F. Sharpey-Schafer, J. Phys. G (London) 2, 249 (1976).

[8]N. G. Alenius, O. Skeppstedt, and E. Wallander, Phys. Scr. 6, 303 (1972).

[9]P. J. Nolan, L. L. Gadeken, A. J. Brown, P. A. Butler, L. L. Green, A. N. James, J. F. Sharpey-Schafer, and D. A. Viggars, J. Phys. A (London) 7, 1437 (1974).

[10]N. G. Alenius, O. Skeppstedt, and E. Wallander, Phys. Scr. 6, 296 (1972).

[11]L. L. Gadeken, P. J. Nolan, P. A. Butler, L. L. Green, A. N. James, J. P. Sharpey-Schafer, and D. A. Viggars, J. Phys. A (London) 7, 83 (1974); P. J. Nolan, L. L. Gadeken, A. J. Brown, P. A. Butler, L. L. Green, C. J. Lister, A. N. James, J. D. MacArthur, J. F. Sharpey-Schafer, and D. A. Viggars, J. Phys. G (London) 1, 35 (1975).

[12]J. J. Kolata, Ph. Gorodetzky, J. W. Olness, A. R. Poletti, and E. K. Warburton, Phys. Rev. C 9, 953 (1974).

[13]A. R. Poletti, E. K. Warburton, J. W. Olness, J. J. Kolata, and Ph. Gorodetzky, Phys. Rev. C 13, 1180 (1976).

[14]J. J. Kolata, J. W. Olness, E. K. Warburton, and A. R. Poletti, Phys. Rev. C 13, 1944 (1976).

[15]P. M. Endt and C. van der Leun, Nucl. Phys. A214, 1 (1973).

[16]R. Rascher, K. P. Lieb, and M. Uhrmacher, in Symposium of Nuclear Structure, Balatonfüred, Hungary, 1975 (unpublished); J. Keinonen, R. Rascher, M. Uhrmacher, N. Wüst, and K. P. Lieb (unpublished).

[17]F. Brandolini, M. de Poli, and C. Rossi-Alvarez, Nuovo Cimento Lett. 8, 342 (1973).

[18]H. Nann, W. S. Chien, A. Saha, and B. H. Wildenthal, Phys. Lett. 60B, 32 (1975); H. Nann (private communication).

[19]J. Dauk, K. P. Lieb, and A. M. Kleinfield, Nucl. Phys. A241, 170 (1975).

[20]A detailed manual for the practical application of these criteria is given by P. Taras and B. Haas, Nucl. Instrum. Methods 123, 73 (1975).

[21]See, e.g., D. B. Fossan and E. K. Warburton, in *Nuclear Spectroscopy and Reactions, Part C*, edited by J. Cerny (Academic, New York, 1974).

[22]G. J. Costa, T. K. Alexander, J. S. Forster, A. B. McDonald, and I. S. Towner, Nucl. Phys. A256, 277 (1976).

[23]R. Sherr, R. Kouzes, and R. Del Vecchio, Bull. Am. Phys. Soc. 19, 499 (1974); Phys. Lett. 52B, 401 (1974).

[24]R. K. Bansal and J. B. French, Phys. Lett. 11, 145 (1964).

[25]A. M. Bernstein, Ann. Phys. (N.Y.) 69, 19 (1972).

[26]R. Sherr and G. Bertsch, Phys. Rev. C 12, 1671 (1975).

[27]We use the notation $d_{3/2}^{-m}$ and $f_{7/2}^{n}$ to stand for the full $(s, d)^{-m}$ and $(f, p)^{n}$ space. The implication is that the most important components of the wave functions are $d_{3/2}^{-m}$ and $f_{7/2}^{n}$.

[28]E. K. Warburton, J. W. Olness, J. J. Kolata, and A. R. Poletti, Phys. Rev. C 3, 1762 (1976).

[29]J. J. Simpson, S. J. Wilson, P. W. Green, J. A. Kuehner, W. R. Dixon, and R. S. Storey, Phys. Rev. Lett. 35, 23 (1975).

[30]A.M. Nathan and J. J. Kolata Phys. Rev. C 14, 171 (1976).

[31]The p, n, and α separation energies of ^{36}Cl are 7.97, 8.58, and 7.64 MeV, respectively. However, the angular momentum barrier for a state of $J^\pi = 11^-$ would be sufficient to render γ emission competitive with particle emission for several MeV above these energies. Note that the ^{35}Cl 8.84-MeV $J^\pi = \frac{17}{2}^+$ level is nearly 2.5 MeV above the proton separation energy.

[32]B. E. Cooke, R. L. Kozub, W. McLatchie, T. K. Alexander, J. S. Forster, C. Broude, and J. R. Beene, J. Phys. G2, 131 (1976).

[33]D. A. Hutcheon, D. C. S. White, W. J. McDonald, and G. C. Nielsen, Can. J. Phys. 52, 1090 (1974).

[34]J. C. Merdinger, N. Schulz, M. Toulemonde, J. Phys. (Paris) 37, 1 (1976).